Blistering of Langmuir-Blodgett Bilayers Containing Anionic Phospholipids as Observed by Atomic Force Microscopy

Hilde A. Rinia,*# Rudy A. Demel,* Jan P. J. M. van der Eerden,# and Ben de Kruijff*
*Department of Biochemistry of Membranes, Institute of Biomembranes, Centre for Biomembranes and Lipid Enzymology, and #Department of Interfaces, Debye Institute, Utrecht University, Padualaan 8, 3584 CH Utrecht, The Netherlands

ABSTRACT Asymmetric bilayers of different phospholipid compositions have been prepared by the Langmuir-Blodgett (L-B) method, and imaged by atomic force microscopy (AFM). Such bilayers can function as a model for biological membranes. The first leaflet consisted of zwitterionic phospholipids phosphatidylcholine (PC) or phosphatidylethanolamine (PE). The second leaflet consisted of the anionic phospholipid phosphatidylglycerol (PG), in either the condensed or liquid phase or, for comparison, of PC. Different bilayers showed different morphology. In all bilayers defects in the form of holes were present. In some bilayers with a first leaflet consisting of PC, polygonal line-shaped defects were observed, whereas when the first leaflet consisted of PE, mainly round defects were seen. Not only the shape, but also the amount of defects varied, depending on the condition and the composition of the second leaflet. In most of the PG-containing systems the defects were surrounded by elevations, which reversibly disappeared in the presence of divalent cations. This is the first time that such elevations have been observed on phospholipid bilayers. We propose that they are induced by phospholipid exchange between the two leaflets around the defects, leading to the presence of negatively charged phospholipids in the first leaflet. Because the substrate is also negatively charged, the bilayer around the edges is repelled and lifted up. Since it was found that the elevations are indeed detached from the substrate, we refer to this effect as bilayer blistering.

INTRODUCTION

Phospholipid bilayers are commonly used as models for biological membranes. They have been extensively studied by a broad range of techniques, leading to detailed information on both their structure and the molecular orientation of their constituents. During the last decade atomic force microscopy (AFM; Binnig et al., 1986) has proven to be a useful additional method to elucidate the structure of supported phospholipid bilayers (Shao et al., 1996). The main advantage of AFM is that it can provide high-resolution information on the surface of samples under aqueous and physiological conditions (Engel, 1991; Bustamante et al., 1994; Hansma and Hoh, 1994; Lal and John, 1994).

Images have been made of phospholipid bilayers in the condensed phase (Hui et al., 1995; Mou et al., 1995), liquid phase (Rädler et al., 1994) and of phase-separated bilayers (Mou et al., 1995). Also ripple phases (Mou et al., 1994a; Czajkowsky et al., 1995) and domains of interdigitated phospholipids (Mou et al., 1994b) have been observed by AFM. A common feature of supported phospholipid bilayers is the presence of defects in the form of holes in the bilayer. These defects can be used to measure the bilayer thickness, which is typically in the order of 5–6 nm (Mou et al., 1994a, b, 1995; Czajkowsky et al., 1995; Hui et al., 1995; Beckmann et al., 1998).

Molecular resolution has been obtained on layers of phosphatidylglycerol (PG) on alkylated mica (Egger et al., 1990; Weisenhorn et al., 1991), phosphatidylethanolamine (PE) on alkylated mica (Weisenhorn et al., 1991), and on PE bilayers (Zasadzinski et al., 1991; Hui et al., 1995). On phosphatidylcholine (PC), high resolution was achieved after manipulating the bilayer by scanning the same area at least four times with a force of 1 nN. Ridges appeared perpendicular to the scan direction with a spacing of 0.63–0.68 nm (Beckmann et al., 1998).

AFM offers prospects to reveal the surface organization of membrane-associated proteins. For membrane-embedded proteins the first promising results have been published already (Hoh et al., 1993; Karrasch et al., 1994; Yang et al., 1993; Mou et al., 1995; Müller et al., 1995; Sommer et al., 1997; for a review see Engel et al., 1997). However, many proteins associate with membranes via interactions with anionic phospholipids (for a recent review see van Klompenburg and de Kruijff, 1998). To study such proteins, it is important to be able to prepare and analyze supported bilayers containing anionic phospholipids.

There are two established methods used to prepare a supported phospholipid bilayer (Shao et al., 1996). One is vesicle fusion and has been described previously (Brian and McConnell, 1984; Mou et al., 1994a). With this method, a droplet of suspension of phospholipid vesicles is deposited on substrates like glass, mica, or silicon wafer. After adsorption of the vesicles on the substrate they spontaneously form a bilayer. Then, excess vesicles are washed away, leaving a symmetric phospholipid bilayer. Due to electrostatic repulsive forces it will be difficult, if not impossible, to prepare bilayers of negatively charged lipids by vesicle fusion in the absence of divalent cations.

Received for publication 12 November 1998 and in final form 25 May 1999.

Address reprint requests to Dr. Hilde A. Rinia, CBLE, Utrecht University, P.O. Box 80054, Padualaan 8, 3508 TB Utrecht, The Netherlands. Tel.: 31 30 2535512; Fax: 31 30 2522478; E-mail: H.Rinia@chem.uu.nl.

0006-3495/99/09/1683/11 $2.00

Another method used to prepare supported bilayers is the Langmuir-Blodgett (L-B) method, developed by Katharine Blodgett (1935). After spreading a monolayer on a subphase in a Langmuir trough, the monolayer can be deposited on a substrate by pulling this substrate up through the air-water interface, from the aqueous phase into the air. A second layer can be deposited by dipping the substrate, coated with a monolayer, through the air-water interface again, from the air into the aqueous phase (Roberts, 1990).

With the L-B method asymmetric bilayers can be prepared, of which the first leaflet is formed by zwitterionic phospholipids and the second by anionic phospholipids, potentially available for interaction with proteins. The aim of this study was to prepare such asymmetric bilayers and analyze them by AFM. We selected PG as anionic phospholipid because it is a common anionic membrane lipid, known to anchor proteins such as the translocation motor protein SecA (Breukink et al., 1992). The lipid composition of both leaflets was varied as well as the ionic strength of the solution.

MATERIALS AND METHODS

Materials

1,2-Dipalmitoyl-*sn*-glycero-3-phosphocholine (DPPC), 1,2-dimyristoyl-*sn*-glycero-3-phosphoethanolamine (DMPE), 1,2-dimyristoyl-*sn*-glycero-3-[phospho-*rac*-(1-glycerol)] (DMPG), 1,2-dipalmitoyl-*sn*-glycero-3-[phospho-*rac*-(1-glycerol)] (DPPG), 1,2-dioleoyl-*sn*-glycero-3-[phospho-*rac*-(1-glycerol)] (DOPG), 1,2-dimyristoyl-*sn*-glycero-3-[phospho-L-serine] (DMPS), and 1,2-dipalmitoyl-*sn*-glycero-3-[phospho-L-serine] (DPPS) were purchased from Avanti Polar Lipids (Alabaster, AL) and were used without further purification. For all experiments MilliQ water (18.2 MΩ) was used.

Silicon (100) p-type wafers (Wacker-chemitronic GMBH, Germany) were cut in squares of 1×1 cm^2 and cleaned in a mixture of 95–97% H_2SO_4 and 35% H_2O_2 (1:1; v/v). The surface was hydrophilized by boiling for 5 min in a mixture of 25% NH_4OH and 35% H_2O_2 (1:1; v/v), and rinsed with water.

L-B transfer

For the L-B experiments, a home-built trough with a volume of 65 ml and an operational area of 5×13 cm^2 was used, with a well to collect the substrates on which a bilayer was transferred. The surface tension of the spread monolayer on the trough was measured with a platinum Wilhelmy plate connected to a Cahn microbalance (Demel, 1994).

The first leaflet of the bilayer (headgroups toward the substrate) was deposited by transferring a monolayer of DPPC or DMPE with a surface pressure of 35 mN/m from a pure water subphase, onto a silicon substrate, on the upstroke. Before deposition of a second leaflet, some of these monolayers were investigated by AFM in contact mode, in air.

The second leaflet of the bilayer (headgroups toward the aqueous phase) was deposited by transferring a monolayer of DPPC, DPPG, or DOPG at a surface pressure of 26 mN/m from a subphase of 10 mM Tris and 100 mM NaCl, pH 7.4, on the downstroke. A concentration of 10 mM Tris is too small to cause a ripple phase (Mou et al., 1994a). DMPG was deposited at a surface pressure of 22 mN/m or 35 mN/m. DPPS and DMPS were transferred at a surface pressure of 26 mN/m and 35 mN/m, respectively. The monolayers used to form the second leaflet were left to equilibrate on the trough for 1 h before deposition. The transfer speed was 4.7 mm/min. With a moveable barrier, surface pressures were kept constant during transfer. The transfer ratios (the transfer of the second layer relative to the transfer of the first layer) varied between 0.5 and 1. After deposition of the second leaflet, the samples were vertically lowered in a well in the trough. After removal of the phospholipid monolayer from the surface, the substrate with the bilayer was kept under water and positioned horizontally on the bottom of the trough with the bilayer side up. Then an O-ring was put on the substrate, kept in place with some vacuum grease. After this, the substrates could easily be taken out of the trough and transferred to the AFM while the bilayer area within the O-ring remained covered with buffer. All bilayers were made at room temperature and, unless stated otherwise, imaged within 4 h after deposition.

AFM measurements

The bilayer bearing silicon substrate was affixed to a metal disk and mounted on the E-scanner, which was calibrated on a standard grid of 1×1 μm, of a Nanoscope III (Digital Instruments, Santa Barbara, CA). The AFM head with a quartz flow cell was placed over the sample such that the circular slit in the flow-cell fell over the O-ring. Sometimes the O-ring was removed, because we found that it can give rise to distorted images. Care was taken that the bilayer was not exposed to air. After removal of the O-ring the surface tension of the buffer usually kept a droplet on the bilayer in its place. Undistorted measurements with the O-ring gave identical results compared with the measurements without the O-ring.

Oxide-sharpened tips with a spring constant of 0.06 N/m, as estimated by the manufacturer, were used (Digital Instruments, Santa Barbara, CA). Images were obtained while scanning with a scan speed of 4 lines/s, in contact mode. We found that scanning in tapping mode did not give better images than those in contact mode. During scanning the force was set such that it was as small as possible while the image was stable and clear, which was usually at a force smaller than 0.5 nN. Scanning at larger forces damaged the scanned area of the bilayer. Tip-induced defects were created by scanning a part of the bilayer at high speed (60 lines/s), using a force of 10 nN.

The Nanoscope software offers the possibility to study vertical linear cross-sections and height distributions of images. Vertical linear cross-sections gave estimations for the height of a bilayer, using the largest defects, already present in the bilayer. The defects in the different bilayers varied in amount and size, leading to different fractions of uncovered substrate. These fractions were quantified using height distributions. The values given in the Results section are the means $\pm$ the standard deviations.

To examine the influence of divalent cations and the ionic strength of the buffer on the bilayer, in some experiments the buffer above the sample in the flow-cell was replaced by 10 mM Tris, 100 mM NaCl, and 3 mM $MeCl_2$, pH 7.4 (Me^{2+} = Mg^{2+}, Ca^{2+}, Ba^{2+}, or Sr^{2+}) or by 10 mM Tris, 300 mM NaCl, pH 7.4.

RESULTS

PC and PE are common membrane lipids that can be anchored to hydrophilic substrates via their zwitterionic headgroups (Grandbois et al., 1998; Hui et al., 1995). The bilayers we studied always had a first leaflet (headgroups toward the substrate) consisting of DPPC or DMPE, both in the condensed phase. DPPC and DMPE monolayers were imaged with AFM in air (Figs. 1 *A* and 2 *A*, respectively) and in general they looked smooth with a few small defects. The second leaflet of the bilayers (headgroups toward the aqueous phase) consisted of DPPC (for control purposes), or the negatively charged phospholipids DPPG, DMPG, or DOPG. At room temperature and at a surface pressure of 26 mN/m, a monolayer of DPPG is in the condensed phase and of DOPG in the liquid phase. At room temperature, and at a surface pressure of 35 mN/m, a monolayer of DMPG is in

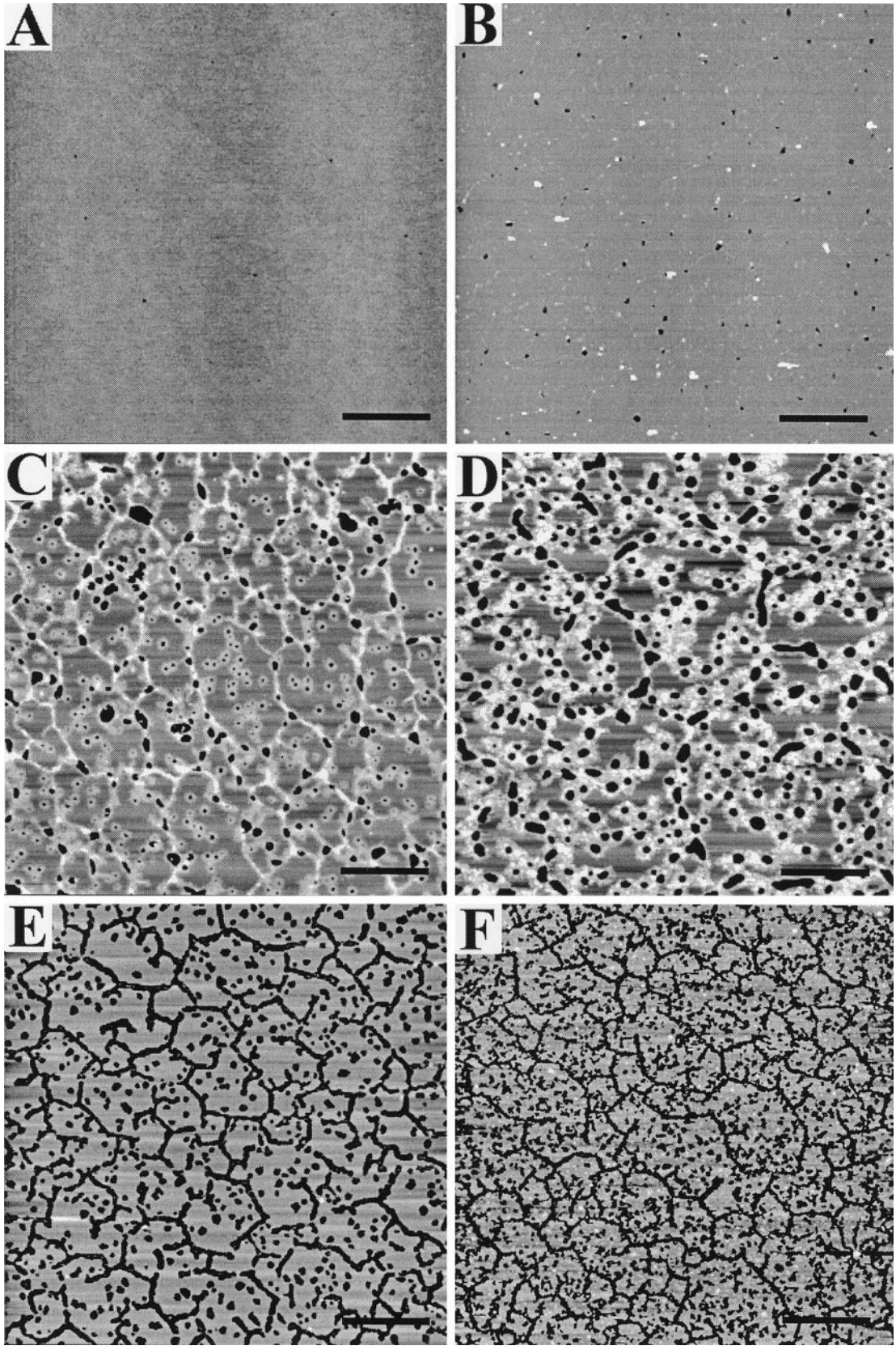

FIGURE 1 Morphology of L-B phospholipid layers. (*A*) Monolayer of DPPC (condensed), transferred from water at a surface pressure of 35 mN/m. Such a monolayer was used as the first leaflet of the following bilayers, of which the second leaflet was transferred from 10 mM Tris buffer, with 100 mM NaCl, pH 7.4, and consisted of (*B*) DPPC deposited at a surface pressure π of 26 mN/m (condensed); (*C*) DPPG deposited at $\pi = 26$ mN/m (condensed); (*D*) DMPG deposited at $\pi = 35$ mN/m (condensed); (*E*) DMPG deposited at $\pi = 22$ mN/m (liquid); and (*F*) DOPG deposited at $\pi = 26$ mN/m (liquid). All images are 10×10 μm; size bar 2 μm; z-scale is 10 nm.

the condensed phase, whereas at a surface pressure of 22 mN/m, it is in the liquid phase. The phases of the monolayers were confirmed by π-A measurements. We selected these different PG lipids and different surface pressures to be able to examine the influence of the packing of the second leaflet on the morphology of the bilayer.

In the following text we refer to the phases of the leaflets of L-B bilayers as those of the monolayer on the trough, before deposition on the substrate. Also, in this paper we refer to an asymmetric bilayer with, for example, DPPC as the first leaflet and DPPG as the second, as DPPC/DPPG.

Bilayers with a first leaflet of DPPC

Fig. 1 *B* shows a typical AFM image of a DPPC/DPPC bilayer (both leaflets in the condensed phase). DPPC/DPPC bilayers in general looked smooth, with some defects (the fraction of uncovered substrate was 6 ± 1%) and quite often, some debris was seen on top of the bilayer. The bilayer height was found to be 6.0 ± 0.1 nm. These results are consistent with what has been found previously (Mou et al., 1994b; Fang and Yang, 1997; Grandbois et al., 1998).

Fig. 1 *C* is a representative image of a DPPC/DPPG bilayer. This image differs distinctively from those obtained on the symmetric DPPC/DPPC bilayer. There are both round and irregularly shaped defects in the DPPC/DPPG bilayer and these defects are always surrounded by elevations. The fraction of uncovered substrate was found to be 8 ± 2%, which is slightly higher compared with the DPPC/DPPC bilayer. A mesh-like, polygonal structure can be seen on the bilayer, which seems to connect the irregular shaped defects. The height of the DPPC/DPPG bilayers was found to be 5.9 ± 0.3 nm. The height of the elevations around the defects varied between 1.5 and 2.5 nm, and the height of the mesh-like structure varied between 2 and 6 nm, taking the bilayer surface as the zero level. The precise heights of these elevations depended on the applied force during scanning. This also applies to the height of elevations on other investigated bilayers, discussed in the next sections.

Similar features were observed for a bilayer with a second leaflet of DMPG in the condensed phase, as is DPPG (Fig. 1 *D*). Again, irregularly shaped defects are present and elevations can be seen on the bilayer. These elevations usually surround the defects, but not as explicitly as in the case of DPPC/DPPG bilayers. The height of these elevations on the bilayer varied between 2 and 3 nm, taking the bilayer surface as the zero level. The height of the DPPC/DMPG (condensed) bilayer was found to be 6.0 ± 0.5 nm, and 15 ± 3% of the substrate was uncovered.

A typical image of a bilayer with DPPC as the first leaflet and DMPG in the liquid phase as the second leaflet is depicted in Fig. 1 *E*. Unlike the DPPC/DMPG (condensed) bilayer, no elevations can be seen on the surface, apart from some debris. There are line-shaped, polygonal defects and some small irregularly shaped defects in these bilayers. The fraction of uncovered substrate was 21 ± 4%, and the height of the DPPC/DMPG (liquid) bilayer was 6.0 ± 0.3 nm.

DPPC/DOPG bilayers (DOPG in the liquid phase) gave similar results, as shown in Fig. 1 *F*. There are line-shaped polygonal and irregularly shaped defects in the bilayers, but the polygonal defects seem more irregular and branched compared to the ones in the DPPC/DMPG (liquid) bilayer. Again, some debris can be seen on the bilayer. DPPC/DOPG bilayers seemed soft under the AFM tip and sometimes it was difficult to get a stable image. The bilayer height was found to be 6.1 ± 0.4 nm, and 24 ± 4% of the substrate was uncovered.

Bilayers with a first leaflet of DMPE

Fig. 2 *B* is an image of a DMPE/DPPC bilayer (both leaflets in the condensed phase). This asymmetrical bilayer of zwitterionic lipids looks smooth, with only a few defects (the fraction of uncovered substrate was 7 ± 5%) and there is less debris on top than on the DPPC/DPPC bilayer (Fig. 1 *B*). The height of this bilayer was found to be 5.6 ± 0.3 nm.

When DPPG (in the condensed phase) was deposited as a second leaflet on a DMPE layer, some of the striking features of the DPPC/DPPG bilayer were observed again, but also some differences were noticed (Fig. 2 *C*). In the DMPE/DPPG bilayer many round defects can be seen with elevations around them. Their height varied between 2 and 3 nm, the bilayer height was found to be 6.0 ± 0.2 nm, and the fraction of uncovered substrate 7 ± 2%. In contradiction to a DPPC/DPPG bilayer (Fig. 1 *C*), there are no mesh-like, polygonal elevations on, and no irregular defects in the DMPE/DPPG bilayer.

Similar images were obtained for the DMPE/DMPG (condensed) bilayer (Fig. 2 *D*). Here the elevations around the round defects are very widespread. Only in some places can the darker gray level of the bilayer be seen, indicated by an arrow. Where the defects are not perfectly round, it seems like two round defects have coalesced. The bilayer was 6.4 ± 0.5 nm high, the elevations were between 2 and 3 nm high, and 10 ± 1% of the substrate was uncovered. Compared with the DPPC/DMPG (condensed) bilayer (Fig. 1 *D*), the defects are rounder and the elevations are more widespread.

When the second leaflet of DMPG in the liquid phase is deposited on DMPE, round defects are again present in the bilayer surrounded by elevations of ~2.5–3.5 nm, as can be seen in Fig. 2 *E*. The elevations are not as widespread, and there are more defects (17% uncovered substrate) in the bilayer compared with DMPG in the solid phase (Fig. 2 *D*). The thickness of the DMPE/DMPG (liquid) bilayer was found to be 5.3 ± 0.1 nm.

Fig. 2 *F* depicts a DMPE/DOPG bilayer (DOPG in the liquid phase) which shows irregular defects in the bilayer and elevations randomly on the bilayer. As in the case of DPPC/DOPG, the layer was easily damaged and it was hard to get a stable image. It appeared that under some elevations defects were present which were only seen after scanning the bilayer surface two or three times or when the force was

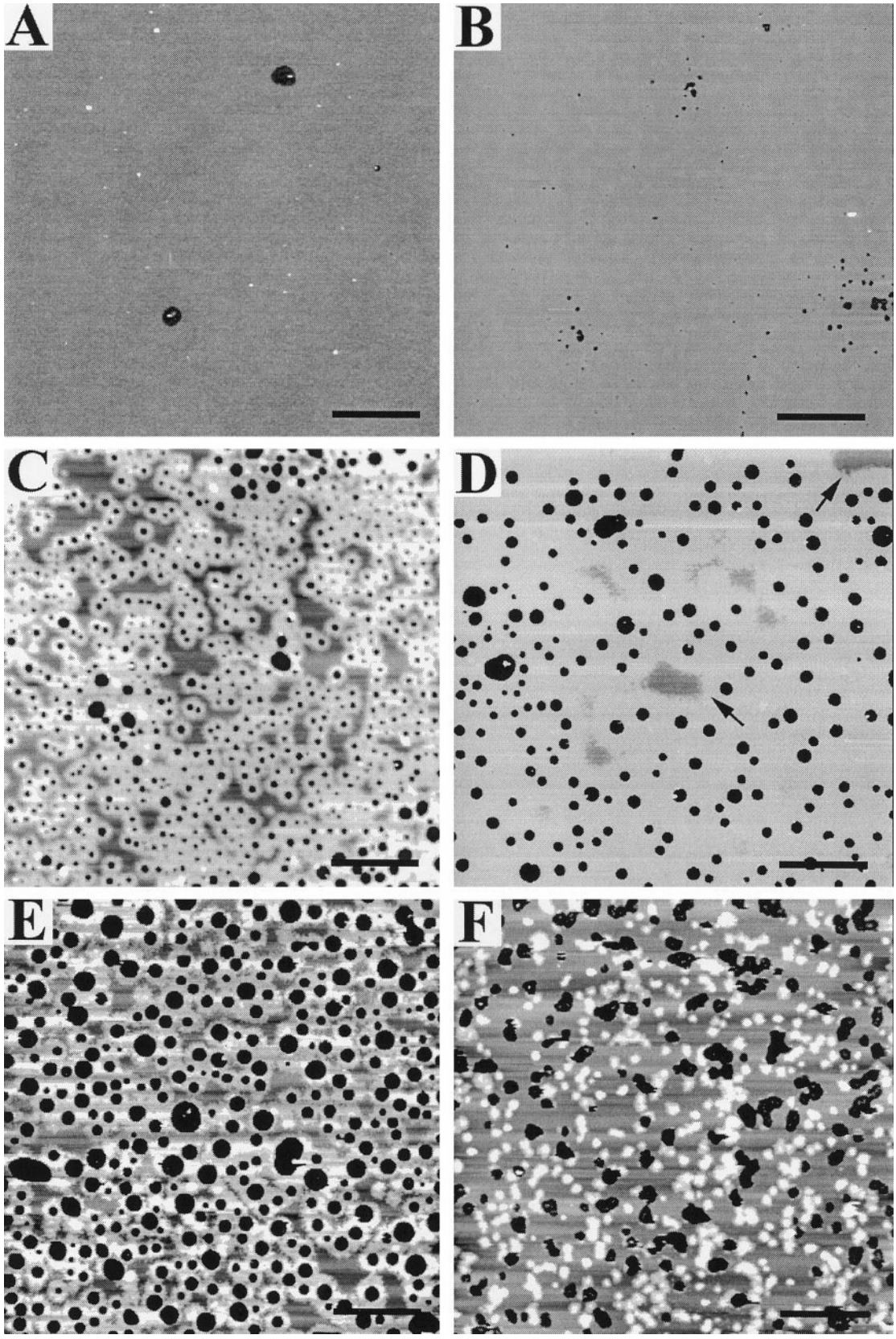

FIGURE 2 (*A*) Monolayer of DMPE, transferred from water at a surface pressure of 35 mN/m (condensed). Such a monolayer was used as the first leaflet of the following bilayers, of which the second leaflet was transferred from 10 mM Tris buffer, with 100 mM NaCl, pH 7.4, and consisted of (*B*) DPPC deposited at a surface pressure π of 26 mN/m (condensed); (*C*) DPPG deposited at π = 26 mN/m (condensed); (*D*) DMPG deposited at π = 35 mN/m (condensed); (*E*) DMPG deposited at π = 22 mN/m (liquid); and (*F*) DOPG deposited at π = 26 mN/m (liquid). All images are 10 × 10 μm; size bar 2 μm; z-scale is 10 nm.

increased a bit (~0.1 nN). This dual character of defects sometimes appearing as holes and sometimes as elevations made it difficult to determine the fraction of uncovered substrate, which was estimated to be 16 ± 9%. The height of the elevations varied between 1.5 and 3 nm and the bilayer was 5.2 ± 0.4 nm high.

It is striking that when PG in the liquid phase is deposited on DMPE (Fig. 2, *E* and *F*), there are elevations present and no line-shaped, polygonal defects can be seen, whereas when PG is deposited on DPPC (Fig. 1, *E* and *F*), there are no elevations on the bilayer and the defects mainly have a line-shaped polygonal character.

About the elevations

To acquire more information on the nature of the elevations present on most of the bilayers with a second leaflet consisting of PG, we studied the influence of the scanning force, time, and ionic composition of the buffer on the appearance of the bilayers, and we introduced tip-induced defects. To determine whether the elevations are induced by the negatively charged headgroups of anionic phospholipids in general or they are specific for PG, we also imaged bilayers with a second leaflet consisting of a different anionic phospholipid, phosphatidylserine (PS).

By increasing the force applied by the tip (to ~1.5 nN), while scanning a DPPC/DPPG bilayer, the height of the elevations could be reduced until almost zero. When afterward the same area was scanned at minimal force, the elevations were again clearly visible, although their height was slightly reduced compared with the height in the initial scan (data not shown). Apparently the elevations can be reversibly pushed down.

After leaving a DPPC/DPPG bilayer overnight (20 h after deposition), both the polygonal elevations and the elevations around the defects had spread out, giving the bilayer an appearance comparable to that of a DPPC/DMPG (condensed) bilayer (Fig. 1 *D*). The elevations usually surround the defects already present in the bilayer. To examine the involvement of defects in the formation of elevations, defects were induced with the AFM tip in a DPPC/DPPG bilayer. After leaving the damaged bilayer overnight, these self-made defects were almost completely surrounded by elevations (data not shown).

All images described so far were obtained by scanning under a 10 mM Tris buffer with 100 mM NaCl, pH 7.4. We also studied some of the systems in the presence of Mg^{2+} or an increased NaCl concentration. These conditions will lead to an increased screening of the surface charge on the bilayer and possibly direct electrostatic interactions.

We imaged the DPPC/DPPG and the DMPE/DMPG (condensed and liquid) bilayers in the presence of Mg^{2+} and found that under these conditions the elevations are absent. This is illustrated in Fig. 3, *A–C*, for a DPPC/DPPG bilayer. Fig. 3 *A* depicts the control situation. After replacing the buffer in the flowcell by a 10 mM Tris buffer with 100 mM NaCl and 3 mM $MgCl_2$, pH 7.4, the elevations had completely disappeared (Fig. 3 *B*). This process is reversible since after replacing the Tris buffer with Mg^{2+} by Tris buffer without Mg^{2+}, the elevations reappeared at the same places (Fig. 3 *C*). When the same DPPC/DPPG bilayer was scanned under 10 mM Tris buffer with 300 mM NaCl, pH 7.4, the elevations became somewhat hazy (Fig. 3 *D*). After replacing this buffer by 10 mM Tris with 100 mM NaCl and 3 mM $MgCl_2$, pH 7.4, the elevations had disappeared again (results not shown).

Note that all images in Fig. 3 are taken on the same area of the DPPC/DPPG bilayer. The pattern of defects remained stable, although due to the repeated scanning the defects became slightly larger. Apparently the tip removed lipids from the edges of the defects. The haziness of the elevations in Fig. 3 *D* is not due to replacing the fluid or scanning the same bilayer several times, because on a different DPPC/DPPG bilayer we determined the influence of 300 mM NaCl straight away and we found the same effect. After replacing the Tris buffer with 300 mM NaCl by Tris buffer with 100 mM NaCl, the elevations had lost their haziness (results not shown).

To determine whether this effect is specific for Mg^{2+}, we imaged DPPC/DPPG and DMPE/DMPG bilayers under buffer (10 mM Tris, 100 mM NaCl, pH7.4) containing 3 mM Ca^{2+}, Ba^{2+}, or Sr^{2+}, and found qualitatively the same results, namely that in the presence of these divalent cations the elevations reversibly disappear. This suggests that the disappearance of the elevations is not the result of specific interactions of PG with Mg^{2+}. Also on DMPE/DPPS (condensed) and DMPE/DMPS (condensed) bilayers, elevations were surrounding the defects, which reversibly disappeared in the presence of divalent cations (data not shown). This implies that the presence of elevations is not PG-specific, but is induced by the negative charges on the headgroups of anionic phospholipids. These results indicate that both the formation and the reversible disappearance of the elevations are governed by electrostatic interactions.

DISCUSSION

In this study, AFM images of asymmetric phospholipid bilayers, of which the second leaflet consists of anionic phospholipids, are presented. The results show that in all the systems in which the second leaflet consists of PG, defects in the shape of holes are present, often surrounded by elevations. Defects in phospholipid L-B bilayers have been observed earlier (Hui et al., 1995; Mou et al., 1995; Czajkowsky et al., 1995; Bassereau and Pincet, 1997; Grandbois et al., 1998). However, to our knowledge, the presence of elevations surrounding the defects has never been reported before.

Bilayers with a second leaflet of PG have been studied with respect to ripple phases, induced by the constituents of PBS buffer (Czajkowsky et al., 1995). We never observed a ripple phase in our systems, which is probably due to the

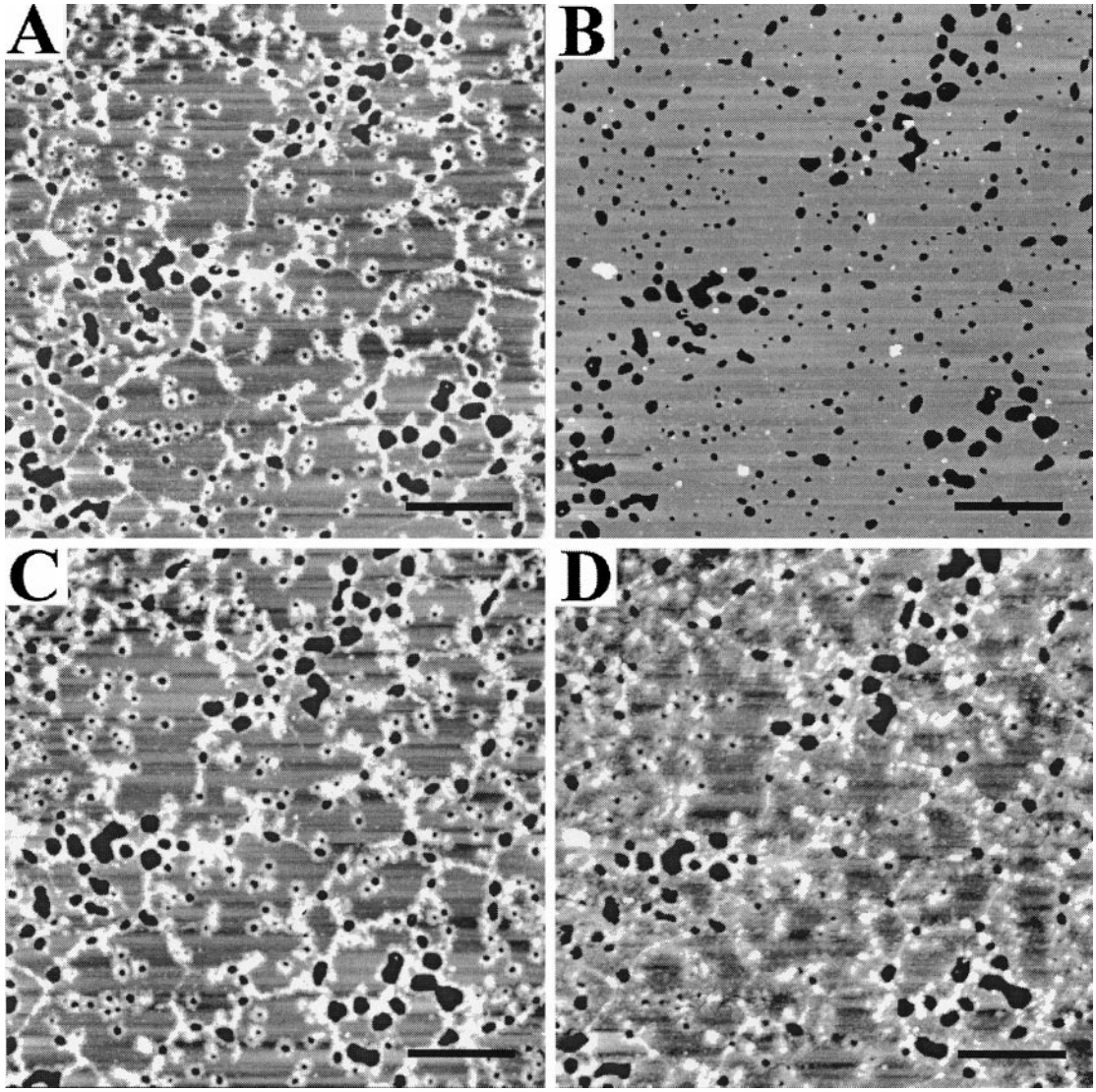

FIGURE 3 The effect of changes in ionic conditions on the morphology of a phospholipid bilayer. On a DPPC/DPPG bilayer (condensed) scanned under (*A*) 10 mM Tris, 100 mM NaCl, pH 7.4, elevations can be seen; (*B*) 10 mM Tris, 100 mM NaCl with 3 mM $MgCl_2$, the elevations have disappeared; (*C*) 10 mM Tris, 100 mM NaCl, pH 7.4, the elevations have reappeared; and (*D*) 10 mM Tris, 300 mM NaCl, pH 7.4, the elevations have become somewhat hazy, but are still present. All images are 5 × 5 μm; size bar 1 μm; z-scale is 10 nm.

fact that we deposited the leaflets at a lower surface pressure and worked with different buffers.

Defects perforating the bilayer are commonly observed in supported phospholipid bilayers (Shao et al., 1996; Bassereau and Pincet, 1997). Our study shows that, in agreement with previous results (Czajkowsky et al., 1995; Mou et al., 1995), defects tunneling both leaflets are also present in L-B bilayers with a second leaflet of anionic phospholipids. The presence of holes in phospholipid bilayers is surprising because the same lipid systems self-assemble in aqueous solution into tightly sealed vesicular bilayers. The fact that supported phospholipid monolayers hardly contain any defects (Bassereau and Pincet, 1997; Figs. 1 *A* and 2 *A*) makes the presence of defects in supported bilayers all the more peculiar. The reason why defects are stable and how the boundary between the lipid and aqueous phases in the defects looks on a molecular scale is not yet clear (Fang and Yang, 1997). Recently, Grandbois and co-workers (1998) found that phospholipase A_2 starts degrading a DPPC bilayer at the boundary of the defects, which led them to propose a plausible model for the edge of defects, with the two leaflets curved toward each other forming a convex structure such that only headgroups are exposed to the aqueous phase (see also Fig. 4).

An explanation for the origin of defects in L-B bilayers has been proposed (Bassereau and Pincet, 1997). These authors suggest that during the deposition of the second monolayer on the first, some lipids of the first monolayer desorb from the substrate and move over to the monolayer on the trough. The same authors state, in agreement with Mou et al., that fewer defects appeared when the second leaflet was transferred at higher surface pressures (Basse-

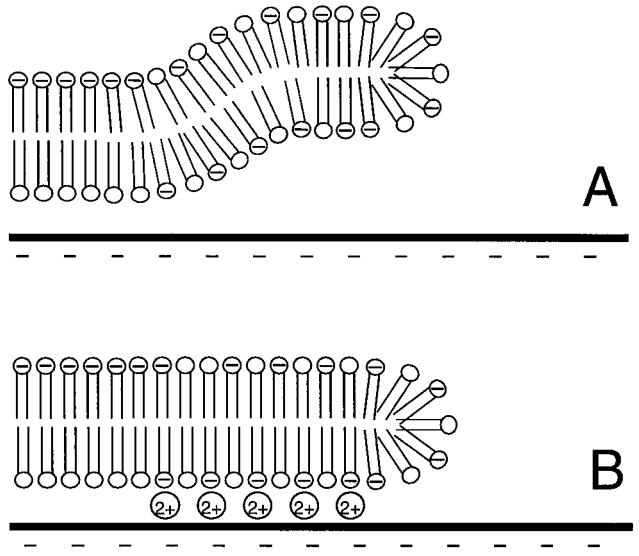

FIGURE 4 Possible molecular model of the elevations around the defects. (*A*) Due to electrostatic repulsion between the negatively charged substrate and anionic phospholipids, present in the first leaflet after lipid exchange, the bilayer edge is lifted up. (*B*) divalent cations screen the surface charges and act as a bridge between the substrate and the first leaflet, forcing the bilayer in a flat conformation.

reau and Pincet, 1997; Mou et al., 1995). We also found that the percentage of uncovered substrate in bilayers with DMPG as a second leaflet, deposited at a high surface pressure (35 mN/m), is lower than in bilayers with DMPG deposited at a low surface pressure (22 mN/m). Moreover, the phase the second leaflet is in also influences the amount of defects, since in the bilayers with PG in the condensed phase (Fig. 1, *C* and *D*; Fig. 2, *C* and *D*), the fraction of uncovered substrate is lower than in bilayers with PG in the liquid phase (Fig. 1, *E* and *F*; Fig. 2, *E* and *F*). Even though the first leaflets of the bilayers depicted in Fig. 1, *B–F* are the same, the amount of uncovered substrate in these bilayers varies, which also counts for Fig. 2, *B–F*. Apparently the conditions of the second leaflet as it is on the trough determine how many lipids leave the substrate during deposition of the second leaflet, which eventually determines the amount of defects in the bilayer.

Not only the amount of the defects in the different bilayers varied, but also the shape of the defects differed, primarily related to the constituents of the first leaflet. In the case of DMPE as the first leaflet, the defects are nearly round, whereas for DPPC as the first leaflet a more irregular pattern was observed. This suggests that it is energetically favorable for DMPE layers to form defects with the lowest boundary-to-uncovered-substrate ratio possible. This might be related to the fact that PE headgroups strongly interact with one another (Hauser et al., 1981).

In all bilayers of which the first leaflet consists of DPPC and the second of PG (Fig. 1, *C–F*), a polygonal structure in the shape of elevations or defects can be seen, even though in the case of DMPG (condensed), it is merely vaguely visible. Interestingly, similar polygonal patterns have been observed by AFM previously in DPPC containing bilayers or monolayers. They appeared in bilayers in which hydrophobic peptides were incorporated (Mou et al., 1996; von Nahmen et al., 1997) and as a phospholipase A_2 hexagonal degradation pattern (Grandbois et al., 1998). These authors suggest that the latter might be due to phospholipase A_2 sensing the hexagonal lattice of the DPPC molecules in the gel phase, or that the enzyme amplifies narrow polygonal defects that are already present in the bilayer.

Apparently, specific properties of PC cause these polygonal patterns in supported bilayers. PC is known to have a bulky headgroup with a larger cross-sectional area than that occupied by two saturated acyl chains. In hydrated bilayers in the condensed phase, this causes packing constraints, resulting in tilted acyl chains (Hauser et al., 1981). We propose that supported DPPC monolayers consist of ordered domains with lipids in a tilted conformation. The direction of the tilt differs from one domain to another and on the borderlines between these domains, disordered line defects are formed which are beyond detection by AFM. From these weak line defects, DPPC molecules preferentially desorb upon passing through the second monolayer on the trough, resulting in a polygonal pattern of defects. In DPPC/DPPC (condensed) bilayers these defects are too narrow to detect, as in the case of DPPC/DPPG (condensed), except here, the elevations give away their presence. When the second leaflet consists of PG in the liquid phase, more lipids desorb from the substrate during deposition of the second leaflet, resulting in wider line defects, detectable by AFM.

We found the most intriguing observation in this study, the presence of the elevations that appeared in most of our systems containing PG. Since these elevations are also observed on bilayers containing PS, but not on bilayers with zwitterionic phospholipids, we presume that they are anionic phospholipid-specific. They formed circular structures surrounding the defects, but they also appeared as a polygonal mesh-like structure on the DPPC/DPPG bilayer. The height of most of the elevations on the PG leaflets varied between 1.5 and 3.5 nm, and the mesh-like elevations were somewhat higher, namely 2–6 nm. The former height suggests that the elevations may be formed by a phospholipid monolayer on top of the bilayer. However, the lipids in such a monolayer would have their tails exposed to either the aqueous phase or the headgroup phase of the underlying bilayer, and both orientations are unstable. Also, the fact that the elevations disappear in the presence of divalent cations and that this process is reversible makes it unlikely that the elevations are material lying on the bilayer.

A possible explanation is that the elevations are artefacts caused by varying surface charge densities, which are known to influence the distance between the negatively charged tip and the surface (Müller and Engel, 1997). Locally higher negative charge densities on a surface would be registered by AFM as elevations, of which the height would decrease with increasing force applied by the tip. At higher ionic strength, surface charges are screened and thus the thickness of the electrical double layer around the charged

surfaces is reduced, lowering the height of the charged surface, as observed by AFM (Müller and Engel, 1997). This could explain the reversible disappearance of the elevations in the presence of divalent cations. However, a higher negative charge density around the defects is impossible since the lipids around the defects cannot be more closely packed than in the bulk of the bilayer. Moreover, in the case of the high concentration of 300 mM NaCl, where the calculated electrical double layer thickness is lower than in the case of 100 mM NaCl with 3 mM $MgCl_2$ (Israelachvili, 1985; Verwey and Overbeek, 1948), the elevations are still visible. In conclusion, we regard it improbable that the nature of the elevations is a local higher negative charge density on the bilayer surface.

We propose that the elevations are induced by the lipid organization around the defects and that they are formed when the bilayer surrounding the defects is lifted up from the substrate, as illustrated in Fig. 4 *A*. We coin the term bilayer blistering for this novel type of bilayer morphology.

According to the model of the lipids bordering the defects, the two leaflets of a bilayer are in contact via the convex curvature of the bilayer edge (see also Fig. 4). Normally, in sealed bilayers without defects, transbilayer movement occurs very slowly with halftimes in the order of days (de Kruijff and van Zoelen, 1978). However, in our system the presence of a connection between the two leaflets at the edge of the defects could locally allow lipid exchange between both leaflets. Because of this exchange, the first leaflet would contain some negatively charged lipids (PG or PS), around the defects. Since the substrate is negatively charged, repulsive forces between the first leaflet and the substrate would be present. As a result of this electrical repulsion, the bilayer is lifted up around the defects (Fig. 4 *A*). In the presence of divalent cations, the edges lie flat on the substrate due to the screening effect of these ions and because a divalent cation might act as a bridge between a negative charge on the substrate and a negatively charged lipid (Fig. 4 *B*). The increased concentration of NaCl theoretically has a larger screening effect, but Na^+ ions cannot form bridges between two negative charges. Thus an increased Na^+ concentration merely results in a more hazy appearance of the elevations.

Increasing the applied force during scanning made it possible to reduce the height of the elevations to almost zero. In the light of the proposed model, the tip pushes, when the force is large enough, the elevated parts of the bilayer down to the surface of the substrate.

Our assumption that the elevations are caused by lipid exchange between the two leaflets, induced by the lipid organization around the defects, is supported by the observation that elevations were also formed around tip-induced defects. Since lipid exchange is a dynamic process, the area of the first leaflet that contains phospholipids from the second leaflet should, according to our model, expand in time. Leaving a bilayer overnight showed that the elevations do indeed spread in time.

If our proposed model holds true, the elevated parts of the bilayer would be repelled by, and therefore detached from, the substrate, while in the presence of divalent cations the same parts would be attached to the support. To examine whether this is the case, we prepared a DMPE/DPPG bilayer and left it for 24 h, yielding a bilayer that consisted almost completely of elevations around the defects (comparable to a DMPE/DMPG (condensed) bilayer (Fig. 2 *D*)). In the presence of Mg^{2+} we isolated a triangular part of the bilayer from the main bilayer by scratching three lines in the shape of the contours of a triangle (Fig. 5 *A*). This isolated part remained on the substrate in the presence of Mg^{2+}. How-

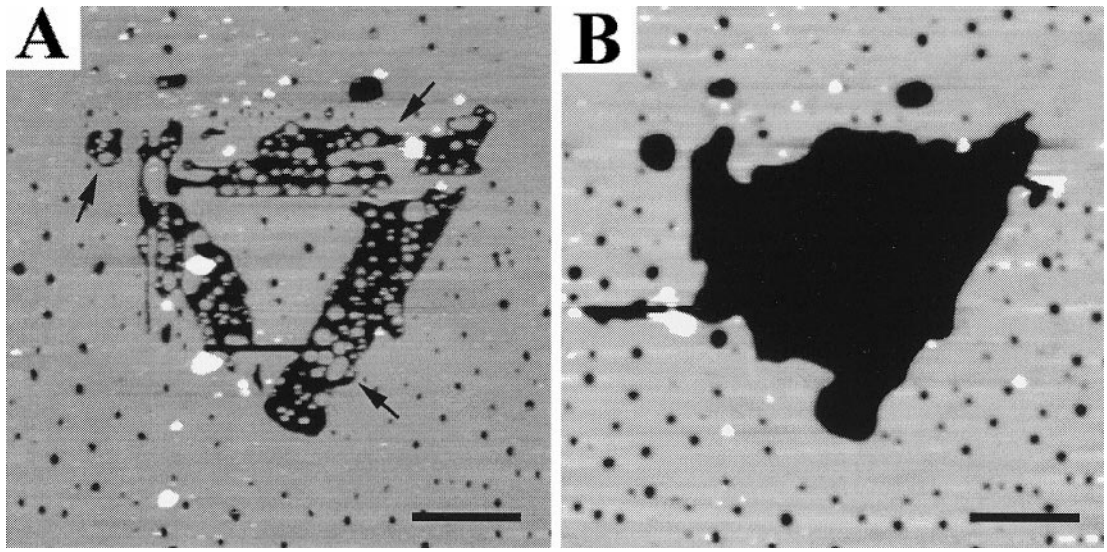

FIGURE 5 Isolation of an elevated part of the bilayer from the main bilayer. A DMPE/DPPG bilayer was left overnight (under 10 mM Tris, 100 mM NaCl, pH 7.4) until it consisted largely of elevations. (*A*) In this bilayer, after the buffer was replaced by 10 mM Tris, 100 mM NaCl, 3 mM $MgCl_2$, pH 7.4, three line defects, contouring a triangle, were scratched with the AFM tip. (*B*) In the absence of Mg^{2+}, the isolated part of the bilayer has disappeared. Both images are 7 × 7 μm; size bar 1.4 μm; z-scale is 10 nm.

ever, after changing the buffer in the flowcell for Tris buffer without Mg^{2+}, the isolated triangle within the scratched lines had disappeared, as can be seen in Fig. 5 *B*. Also, the isolated parts in the scratched lines and other defects (Fig. 5 *A, arrows*) have disappeared in Fig. 5 *B*. This means that the parts of the bilayer that consist of elevations are indeed detached from the support, and that divalent cations can attach these parts on the substrate.

We introduce the phenomenon that the bilayer is locally detached and lifted up from the substrate as bilayer blistering. This bilayer blistering, as we observed by AFM, offers interesting and new possibilities for analysis of lipid-protein interactions.

CONCLUSIONS

In this paper we present AFM images of supported asymmetric bilayers, with a second leaflet consisting of anionic phospholipids (PG). Such systems are of potential interest with respect to studies of membrane-associated proteins. Our results reveal that in our systems with a second leaflet of PG, defects in the form of holes are present. The shape of the defects is influenced primarily by the first leaflet: DPPC as a first leaflet gives rise to irregular or polygonal, line-shaped defects, while DMPE tends to form round defects. In the case of DPPC/DPPG and DPPC/DMPG (condensed) and DMPE/PG bilayers, elevations were observed that disappeared reversibly in the presence of divalent cations. To explain the origin of these elevations and their behavior, we have described a model of the lipidic phase bordering the defects. We propose that, after lipid exchange between the first and the second leaflet, the bilayer edges are lifted up due to repulsive forces between the negatively charged substrate and negatively charged lipids that would be present in the first leaflet, due to the lipid exchange. It was found that the elevations are indeed detached from the surface, which led us to call their formation bilayer blistering.

We thank dr. E ten Grotenhuis and dr. J. C. van Miltenburg for advice concerning AFM, G. J. K. van den Berg and D. Wijnands for technical assistance, and dr. H. E. A. Huitema.

This work was supported by the Division of Chemical Sciences with financial aid from the Netherlands Organization for Scientific Research (N.W.O.).

REFERENCES

Bassereau, P., and F. Pincet. 1997. Quantitative analysis of holes in supported bilayers providing the adsorption energy of surfactants on solid substrates. *Langmuir*. 13:7003–7007.

Beckmann, M., P. Nollert, and H.-A. Kolb. 1998. Manipulation and molecular resolution of a phosphatidylcholine-supported planar bilayer by atomic force microscopy. *J. Membr. Biol.* 161:227–233.

Binnig, G., C. F. Quate, and Ch. Gerber. 1986. Atomic Force Microscope. *Phys. Rev. Lett*. 56:930–933.

Blodgett, K. B. 1935. Films built by depositing successive monomolecular layers on a solid surface. *J. Am. Chem. Soc.* 57:1007–1022.

Breukink, E., R. A. Demel, G. de Korte-Kool, and B. de Kruijff. 1992. SecA insertion into phospholipids in stimulated by negatively charged lipids and inhibited by ATP: a monolayer study. *Biochemistry*. 31: 1119–1124.

Brian, A. A., and H. M. McConnell. 1984. Allogeneic stimulation of cytotoxic T cells by supported planar membranes. *Proc. Natl. Acad. Sci. USA.* 81:6159–6163.

Bustamante, C., D. A. Erie, and D. Keller. 1994. Biochemical and structural applications of scanning force microscopy. *Curr. Opin. Struct. Biol.* 4:750–760.

Czajkowsky, D. M., C. Huang, and Z. Shao. 1995. Ripple phase in asymmetric unilamellar bilayers with saturated and unsaturated phospholipids. *Biochemistry.* 34:12501–12505.

de Kruijff, B., and E. J. J. van Zoelen. 1978. Effect of the phase transition on the transbilayer movement of dimyristoyl phosphatidylcholine in unilamellar vesicles. *Biochim. Biophys. Acta*. 511:105–115.

Demel, R. A. 1994. Monomolecular layers in the study of biomembranes. *Subcellular Biochemistry.* 23:83–120.

Egger, M., F. Ohnesorge, A. L. Weisenhorn, S. P. Heyn, B. Drake, C. B. Prater, S. A. C. Gould, P. K. Hansma, and H. E. Gaub. 1990. Wet lipid-protein membranes imaged at submolecular resolution by atomic force microscopy. *J. Struct. Biol.* 103:89–94.

Engel, A. 1991. Biological applications of scanning probe microscopes. *Annu. Rev. Biophys. Biophys. Chem.* 20:79–108.

Engel, A., C.-A. Schoenenberger, and D. J. Müller. 1997. High resolution imaging of native biological sample surfaces using scanning probe microscopy. *Curr. Opin. Struct. Biol.* 7:279–284.

Fang, Y., and J. Yang. 1997. The growth of bilayer defects and the induction of interdigitated domains in the lipid-loss process of supported phospholipid bilayers. *Biochim. Biophys. Acta*. 1324:309–319.

Grandbois, M., H. Clausen-Schaumann, and H. Gaub. 1998. Atomic force microscope imaging of phospholipid bilayer degradation by phospholipase A_2. *Biophys. J.* 74:2398–2404.

Hansma, H. G., and J. H. Hoh. 1994. Biomolecular imaging with the atomic force microscope. *Annu. Rev. Biophys. Biomol. Struct.* 23: 115–139.

Hauser, H., I. Pascher, R. H. Pearson, and S. Sundell. 1981. Preferred conformation and molecular packing of phosphatidylethanolamine and phosphatidylcholine. *Biochim. Biophys. Acta*. 650:21–51.

Hoh, J. H., G. E. Sosinsky, J.-P. Revel, and P. K. Hansma. 1993. Structure of the extracellular surface of the gap junction by atomic force microscopy. *Biophys. J.* 65:149–163.

Hui, S. W., R. Viswanathan, J. A. Zasadzinski, and J. N. Israelachvili. 1995. The structure and stability of phospholipid bilayers by atomic force microscopy. *Biophys. J.* 68:171–178.

Israelachvili, J. N. 1985. Intermolecular and Surface Forces with Applications to Colloidal and Biological Systems. Academic Press, London.

Karrasch, S., R. Hegerl, J. H. Hoh, W. Baumeister, and A. Engel. 1994. Atomic force microscopy produces faithful high-resolution images on protein surfaces in an aqueous environment. *Proc. Natl. Acad. Sci. USA*. 91:836–838.

Lal, R., and S. A. John. 1994. Biological applications of atomic force microscopy. *Am. J. Physiol.* 266:C1–C21.

Mou, J., D. M. Czajkowsky, and Z. Shao. 1996. Gramicidin A aggregation in supported gel state phosphatidylcholine bilayers. *Biochemistry.* 35: 3222–3226.

Mou, J., J. Yang, C. Huang, and Z. Shao. 1994b. Alcohol induces interdigitated domains in unilamellar phosphatidylcholine bilayers. *Biochemistry.* 33:9981–9985.

Mou, J., J. Yang, and Z. Shao. 1994a. Tris(hydroxymethyl)aminomethane ($C_4H_{11}NO_3$) induced a ripple phase in supported unilamellar phospholipid bilayers. *Biochemistry.* 33:4439–4443.

Mou, J., J. Yang, and Z. Shao. 1995. Atomic force microscopy of cholera toxin B-oligomers bound to bilayers of biologically relevant lipids. *J. Mol. Biol.* 248:507–512.

Müller, D. J., and A. Engel. 1997. The height of biomolecules measured with the atomic force microscope depends on electrostatic interactions. *Biophys. J.* 73:1633–1644.

Müller, D. J., F. A. Schabert, G. Büldt, and A. Engel. 1995. Imaging purple membranes in aqueous solutions at sub-nanometer resolution by atomic force microscopy. *Biophys. J.* 68:1681–1686.

Rädler, J., M. Radmacher, and H. E. Gaub. 1994. Velocity-dependent forces in atomic force microscopy imaging of lipid films. *Langmuir*. 10:3111–3115.

Roberts, G. 1990. Langmuir-Blodgett Films. Plenum Press, New York and London.

Shao, Z., J. Mou, D. M. Czajkowsky, J. Yang, and J.-Y. Yuan. 1996. Biological atomic force microscopy: what is achieved and what is needed. *Adv. Phys.* 45:1–86.

Sommer, F., S. Alexandre, N. Dubreuil, D. Lair, Tran-minh Duc, and J. M. Valleton. 1997. Contribution of lateral force and "tapping mode" microscopies to the study of mixed protein Langmuir-Blodgett films. *Langmuir*. 13:791–795.

van Klompenburg, W., and B. de Kruijff. 1998. The role of anionic lipids in protein insertion and translocation in bacterial membranes. *J. Membr. Biol.* 162:1–7.

Verwey, E. J. W., and J. Th. G. Overbeek. 1948. Theory of the Stability of Lyophobic Colloids. Elsevier Publishing Company, Inc., New York.

von Nahmen, A., M. Schenk, M. Sieber, and M. Amrein. 1997. The structure of a model pulmonary surfactant as revealed by scanning probe microscopy. *Biophys. J.* 72:463–469.

Weisenhorn, A. L., M. Egger, F. Ohnesorge, S. A. C. Gould, S.-P. Heyn, H. G. Hansma, R. L. Sinsheimer, H. E. Gaub, and P. K. Hansma. 1991. Molecular-resolution images of Langmuir-Blodgett films and DNA by atomic force microscopy. *Langmuir*. 7:8–12.

Yang, J., L. K. Tamm, T. W. Tillack, and Z. Shao. 1993. New approach for atomic force microscopy of membrane proteins, the imaging of cholera toxin. *J. Mol. Biol.* 229:286–290.

Zasadzinski, J. A. N., C. A. Helm, M. L. Longo, A. L. Weisenhorn, S. A. C. Gould, and P. K. Hansma. 1991. Atomic force microscopy of hydrated phosphatidylethanolamine bilayers. *Biophys. J.* 59:755–760.